Vibrational dynamics of rutile-type GeO_2 from micro-Raman spectroscopy experiments and first-principles calculations

2015 EPL 109 26007

(http://iopscience.iop.org/0295-5075/109/2/26007)

A Letters Journal Exploring the Frontiers of Physics

January 2015

EPL, **109** (2015) 26007 www.epljournal.org
doi: 10.1209/0295-5075/109/26007

Vibrational dynamics of rutile-type GeO_2 from micro-Raman spectroscopy experiments and first-principles calculations

A. Sanson[1], G. S. Pokrovski[2], M. Giarola[3] and G. Mariotto[3]

[1] *Department of Physics and Astronomy, University of Padova - Via Marzolo 8, 35131 Padova, Italy*
[2] *Groupe Métallogénie Expérimentale, Géosciences Environnement Toulouse GET, University of Toulouse, CNRS - IRD - OMP - Avenue Edouard Belin 14, 31400 Toulouse, France*
[3] *Department of Computer Science, University of Verona - Strada le Grazie 15, 37134 Verona, Italy*

received 4 December 2014; accepted in final form 18 January 2015
published online 3 February 2015

PACS 63.70.+h – Statistical mechanics of lattice vibrations and displacive phase transitions
PACS 78.30.Er – Infrared and Raman spectra: Solid metals and alloys
PACS 78.20.-e – Optical properties of bulk materials and thin films

Abstract – The vibrational dynamics of germanium dioxide in the rutile structure has been investigated by using polarized micro-Raman scattering spectroscopy coupled with first-principles calculations. Raman spectra were carried out in backscattering geometry at room temperature from micro-crystalline samples either unoriented or oriented by means of a micromanipulator, which enabled successful detection and identification of all the Raman active modes expected on the basis of the group theory. In particular, the E_g mode, incorrectly assigned or not detected in the literature, has been definitively observed by us and unambiguously identified at $525\,cm^{-1}$ under excitation by certain laser lines, thus revealing an unusual resonance phenomenon. First-principles calculations within the framework of the density functional theory allow quantifying both wave number and intensity of the Raman vibrational spectra. The excellent agreement between calculated and experimental data corroborates the reliability of our findings.

Introduction. – Germanium dioxide (GeO_2) is a promising candidate for applications especially in optoelectronic devices, owing to its high dielectric constant and refractive index, as well as its large thermal stability [1,2]. Under ambient conditions, GeO_2 exists in two crystallographic phases: the hexagonal α-quartz and the tetragonal rutile-type phase. The latter, whose mineral name is argutite, is the thermodynamically stable polymorph at ambient conditions [3,4]. Its vibrational dynamics is the subject of the present study.

Many experimental and theoretical studies have been conducted on the rutile-phase of GeO_2 to investigate its physical and thermodynamic properties and solubility [5–17]. However, its vibrational properties are not yet fully clarified. In particular, only 3 of the 4 active Raman vibrational modes, expected from the group theory, have been unambiguously observed and reported in literature. Specifically, the detection and the assignment of the expected Raman-active mode with E_g symmetry has been subject of debate over the past forty years. In the first pioneering Raman study of Scott [18], the E_g Raman mode was tentatively referred at $\sim 680\,cm^{-1}$, as a shoulder on the low-frequency side of the A_{1g} mode peaked at $\sim 700\,cm^{-1}$. Later on, other Raman investigations were performed [19–22], but without shedding light on the detection of the E_g Raman mode. For example, Gillet *et al.* [21] observed a weak band at $465\,cm^{-1}$ that was tentatively associated to the missing E_g Raman mode, but the same authors also claimed that this weak band might arise from very small amounts of the GeO_2 hexagonal-type phase also present in the sample. Mernagh and Liu [23], in agreement with Scott, pointed out that the missing E_g mode might be the shoulder of the A_{1g} mode observed at about $684\,cm^{-1}$, but, at the same time, they affirmed that a more likely possibility is that this band may be due to an optically inactive E_u mode which becomes Raman active. Finally, very recently, another vibrational study of rutile-type GeO_2 was performed by Kaindl and co-workers [24], but, again, no evidence was found of the E_g Raman mode.

In this work, we shed light on this issue by unambiguously identifying the E_g mode of rutile-type GeO_2 at about $525\,cm^{-1}$. Moreover, we have found that such weak Raman peak is observed only under some

excitation wavelengths, thus revealing an anomalous resonance phenomenon. To corroborate our experimental findings, first-principles calculations of both wave number and intensity of the Raman vibrational modes have been performed to help spectral band assignment. The overall agreement between experimental results and first-principles calculations is excellent.

Experimental. – Argutite (GeO_2, tetragonal, rutile-like) was synthesized from commercial GeO_2 powder (hexagonal, quartz-like, 99.95% purity, Sigma-Aldrich), as detailed in ref. [16]. The obtained small-size grain (<1 micron) powder of argutite was aged for several weeks in contact with water in a titanium reactor at 250–300 °C and saturated vapour pressure (40–80 bars). Ageing runs were repeated several times, followed each time by rapid quench of the reactor, rinsing the solid and replacing the reaction solution with fresh water. This treatment enabled removal of ultra-small particles and favoured the formation of bigger argutite crystals [17]. Compact crystal agglomerates and crusts of argutite larger than 1 mm in size that formed on the reactor walls were selected for Raman measurements.

Room-temperature polarized Raman spectra were carried out in backscattering geometry from some micro-crystals, whose size was typically ~ 10 micron $\times$ 15 micron, using a microprobe setup consisting of an Olympus microscope BX41 coupled with a triple monochromator (Horiba-Jobin Yvon, model T64000), equipped with holographic gratings, having 1800 lines/mm, and set in double-subtractive/single configuration. The spectra were excited by the 647.1 nm line of a mixed Ar-Kr ion gas laser; selected measurements were also performed at different excitation wavelengths of 454.5, 488.0, 514.5, and 568.2 nm. The scattered radiation, filtered by the fore double monochromator, was recorded by an open-electrode coupled charge device (CCD) detector, with 1024×256 pixels, cooled by liquid nitrogen. The spectral resolution was better than 0.2 cm^{-1}/pixel, when red wavelength was used to excite the spectra, while an accurate wave number calibration of the spectrometer was achieved based on the emission lines of a Ne spectral lamp.

For the polarization analysis of Raman spectra of GeO_2 crystals the Porto's notation [25] was adopted, and, accordingly, the scattering configuration was referred as $\bar{k}_i(\bar{E}_i, \bar{E}_s)\bar{k}_s$, where $\bar{k}_i$ and $\bar{k}_s$ are the propagation directions, while $\bar{E}_i$ and $\bar{E}_s$ are the polarization directions of the incident and scattered light, respectively. With reference to the orthogonal XYZ laboratory frame, in the case of measurements carried out in the backscattering geometry, the propagation directions of both incident and scattered radiation correspond to the same Z-direction. Moreover, in order to have the same laser power at the sample surface, all spectra were excited without modifying the polarization direction of incident laser radiation, and the polarization analysis was ensured by the scattered radiation analyzer, coupled to a scrambler placed at the spectrometer entrance slit.

Repeated micro-Raman measurements were carried out under the same experimental conditions from different micro-regions of the single crystal under investigation, and the spectra showed a very good reproducibility. To this aim, the proper orientation of the single micro-crystal was achieved using a homemade micromanipulator operated under direct optical inspection of a colour camera interfaced to a microscope objective, the same used to focus the laser beam onto the sample. This homemade set-up turned out to have a crucial role in recent vibrational dynamics studies carried out by us on micro-crystalline TiO_2 anantase [26], as well as on crystalline rare earth orthophosphates [27,28] in order to select and identify the different symmetry modes of these crystals. The core of the micromanipulator was a high angular-resolution goniometer, which allowed for very accurate, step-by-step, rotations of the crystal around its crystallographic c-axis.

Computational details. – First-principles calculations, based on density-functional theory within the local density approximation, have been performed to predict the Raman active vibrational modes of rutile-type GeO_2, both in wave number and intensity. The CRYSTAL-14 package was used, a periodic first-principles program that employs a Gaussian-type basis set to describe the crystalline orbitals [29]. All-electron basis sets have been adopted, with 9-766131 contraction (one s, two sp, two d, and two sp shells) for germanium atoms [30], and 8-411 contraction (one s and three sp shells) for oxygen atoms [31,32]. Pure density-functional theory calculations have been carried out using Dirac-Slater [33] exchange and Vosko-Wilk-Nusair [34] correlation functionals. Other exchange-correlation functionals were tested, but among those that are currently available in CRYSTAL-14 to calculate the Raman intensity via the Coupled Perturbed Hartree-Fock/Kohn-Sham method [35], these give better results.

The level of accuracy in evaluating bi-electronic integrals (Coulomb and exchange series) is controlled by five parameters, for which standard values (6 6 6 6 12) were adopted. The self-consistent–field convergence thresholds was set to 10^{-8} Hartree for both total energy and eigenvalues in order to ensure good convergence, while the Brillouin zone integration was computed with a Monkhorst-Pack shrinking factor [36] of 10. The vibrational frequencies at the Γ-point were computed within the harmonic approximation by diagonalizing the mass-weight Hessian matrix, whose (i, j) element is defined as $W_{ij} = H_{ij}/\sqrt{M_i M_i}$ where M_i and M_j are the masses of the ith and jth atoms, respectively. A more complete description of the computational aspects can be found in refs. [37,38]

Results and discussion. – The crystal structure of rutile-type GeO_2 is tetragonal with the space group D_{4h}^{14} ($P42/mnm$), number 136 in the standard listing. The

primitive cell contains two GeO_2 formula units (*i.e.*, six atoms). On the basis of the factor group analysis, the resulting fifteen vibrational degrees of freedom of rutile-type GeO_2 occur as 11 optical modes at the Γ-point of the Brillouin zone, with the following irreducible representation:

$$A_{1g} + A_{2g} + A_{2u} + B_{1g} + B_{2g} + 2B_{1u} + E_g + 3E_u, \quad (1)$$

where the E_g and E_u modes are double degenerated. The four modes A_{2u} and $3E_u$ are IR active, whereas the four modes A_{1g}, B_{1g}, B_{2g} and E_g are Raman active. The remaining three modes A_{2g} and $2B_{1u}$ are inactive (silent). Since no optical mode of rutile-type GeO_2 is double active (*i.e.*, Raman and IR), the transverse optic-longitudinal optic (TO-LO) splitting for the IR active modes does not affect its Raman spectrum. Corresponding to each Raman-active mode of rutile-type GeO_2, there is a scattering tensor having a distinctive symmetry. The expected Raman polarizability tensors turn out to have the following form [39]:

$$\alpha(A_{1g}) = \begin{pmatrix} a & 0 & 0 \\ 0 & a & 0 \\ 0 & 0 & b \end{pmatrix}, \quad (2)$$

$$\alpha(B_{1g}) = \begin{pmatrix} c & 0 & 0 \\ 0 & -c & 0 \\ 0 & 0 & 0 \end{pmatrix}, \quad (3)$$

$$\alpha(B_{2g}) = \begin{pmatrix} 0 & d & 0 \\ d & 0 & 0 \\ 0 & 0 & 0 \end{pmatrix}, \quad (4)$$

$$\alpha(E_g) = \begin{pmatrix} 0 & 0 & e \\ 0 & 0 & e \\ e & e & 0 \end{pmatrix}. \quad (5)$$

The knowledge of these scattering tensors is mandatory for the study of the Raman spectrum of rutile-type GeO_2.

Usually, in order to experimentally examine a given specific component ij of the Raman modes of a single crystal, one merely arranges the scattering experiment in such a way that the incident light is polarized in the "i"-direction while only the scattered light having "j" polarization is observed. Depending on the j and i value either the Raman spectrum of the crystal in parallel or crossed polarization can be observed.

Since the crystal structure of rutile GeO_2 is uniaxial, the determination of the c-axis (z-direction) may be conveniently done optically or by x-rays diffraction. In our case, it was not easy to determine this direction, *i.e.* the c-axis of the GeO_2 microcrystals selected for our Raman measurements, due to their partial inclusion into the pristine polycrystalline agglomerate resulting from the growth process, which most often prevented the possibility to perfectly align the electric field of the incident/scattered radiation along this axis. Nevertheless, after a very patient and accurate selection, fully polarized Raman spectra, excited by laser light polarized either along the crystallographic c-axis or perpendicularly to it, were carried out in back-scattering geometry from some micro-crystals characterized by different growth planes. Three significant experimental spectra, recorded in backscattering geometry and carried out in parallel polarization from two micro-crystals grown along different crystallographic orientations, but both having very flat surfaces exposed to air, and hereafter referred as micro-crystal A and B, respectively, are reported in fig. 1, where the related symmetry attributions are also indicated.

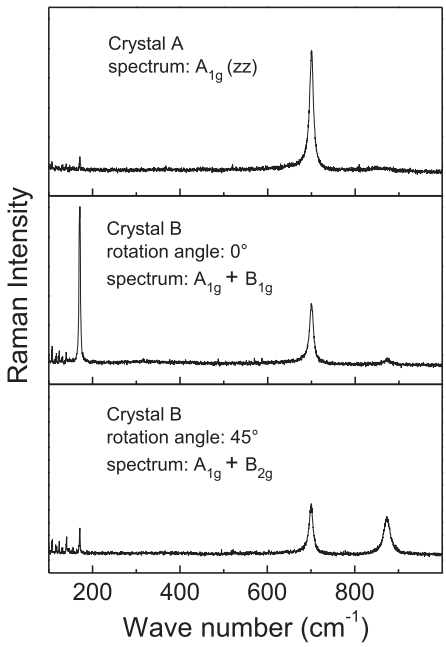

Fig. 1: Experimental Raman spectra recorded from two rutile-type GeO_2 micro-crystals in backscattering geometry under excitation of the 647.1 nm line and observed in the parallel polarization setting $-Z(XX)Z$, where X and Z are a set of two orthogonal axes of the laboratory frame. Refer to the text for the details about the symmetry selection.

The spectrum shown in the top panel of fig. 1, carried out in parallel (XX) polarization from sample A, consists of a single strong peak at about 700 cm^{-1}, even though the presence of a small peak at about 171 cm^{-1} and of a very weak band centred at about 870 cm^{-1} cannot be ruled out. On the basis of the Raman tensors form of this crystal (*i.e.*, eqs. (2) and (3)) and taking into account the polarization setting adopted for our measurements, this spectrum is expected to correspond to the zz component of the A_{1g} mode of rutile-type GeO_2. Therefore, it can be concluded that the electric-field direction of both incident and back-scattered light was aligned along the c-axis of the probed micro-crystal. In fact, in the case of Raman measurements in backscattering geometry carried out in parallel polarization configuration, if the electric-field direction of the laser light does not match this crystallographic c-axis, one should expect, according to eqs. (2) and (3), to observe in the XX parallel polarized spectrum also the B_{1g} mode, together with the A_{1g} one. However, this does not seem to occur for the spectrum plotted in the

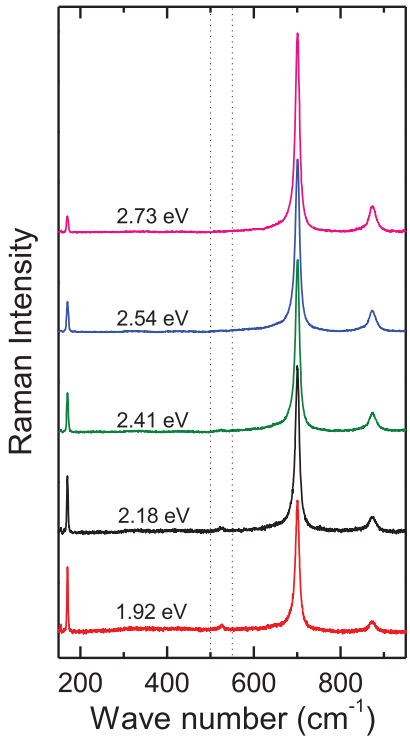

Fig. 2: (Colour on-line) Unpolarized Raman spectra of rutile-type GeO_2 crystals carried out under different excitation energies, quoted just above each spectral profile. Each spectrum is plotted in its relative intensity scale, after normalization to total amplitude between 150 and 950 cm^{-1}. The spectra are offset vertically in order to make clearer the observation of the spectral evolution. The weak peak at about 525 cm^{-1}, clearly observable under excitation of yellow and red excitation lines, is identified as the fourth E_g mode predicted by the group theory.

Table 1: Calculated Born effective charge tensors in rutile-type GeO_2 for the Ge atom at $(0, 0, 0)$ and the O atom at (0.3044, 0.3044, 0) position. The directions xx, yy and zz are along a, b and c in the conventional cell, respectively.

	Ge	O
Z^*_{xx}	+3.992	−1.996
Z^*_{yy}	+3.992	−1.996
Z^*_{zz}	+4.251	−2.125
Z^*_{xy}	+0.470	−0.531

Table 2: Calculated high-frequency and static dielectric tensors in rutile-type GeO_2.

	This study	Ref. [43]
$\epsilon^\infty_{xx} = \epsilon^\infty_{yy}$	3.646	3.679
ϵ^∞_{zz}	4.066	3.945
$\epsilon^0_{xx} = \epsilon^0_{yy}$	7.954	10.876
ϵ^0_{zz}	6.088	8.747

top panel of fig. 1. Therefore, the occurrence of the small peak at about 171 cm^{-1} and that of the hardly observable band at about 870 cm^{-1} suggest a weak spill-over of forbidden modes of this crystal. In the light of the above considerations, it can be concluded that the c-axis of the crystal A belongs to sample surface irradiated by the laser beam.

On the other hand, the spectrum plotted in the middle panel of fig. 1 was also acquired in parallel (XX) polarization from the second micro-crystal (B), after having rotated it step by step around the Z-axis perpendicular to the crystal surface exposed to the laser beam, until the intensity of the mode peaked at about 171 cm^{-1} attained the maximum. In fact, the displayed spectrum shows a strong and sharp peak at ∼171 cm^{-1}, together with the same A_{1g} mode of the crystal, which turns out relatively less intense, while a very weak peak occurs at about 873 cm^{-1}. According to eqs. (3), (4) and on the basis of *ab initio* calculations (see below), this peak should be attributed to the B_{1g} mode, being related to tensor components of the basal plane (in-plane components), perpendicular to crystallographic c-axis. This polarization setting allows as well for simultaneous observation of the A_{1g} mode, which in fact occurs at 700 cm^{-1}, although it has a different (lower) relative intensity with respect to that observed on crystal A, where it was related to tensor component zz, out of the basal plane (see eq. (2)). As for the small peak at about 873 cm^{-1}, it should be due to the weak spill over of the "in-plane" Raman active B_{2g} mode. Finally, the spectrum reported in the bottom panel of fig. 1 was also observed on the crystal B in parallel (XX) polarization, but after a crystal rotation of 45 degrees around the Z-axis direction (*i.e.*, that of the incident laser beam), which maximizes the Raman mode peaked at 873 cm^{-1}, while minimizing the B_{1g} peak, even if this last appreciably spills. However, in this case too, the A_{1g} peak is expected to occur with the same intensity as the previous one, since the intensity of the A_{1g} mode components in the basal plane is independent of the crystal rotation angle around its intrinsic c-axis. This spectrum, according to the transformation rules of Raman tensor components between the laboratory and the intrinsic frames, should be assigned to A_{1g} and B_{2g} modes (*e.g.*, $A_{1g} + B_{2g}$ spectrum). Therefore, on the basis of our experimental observations, it can be concluded that the c-axis of the crystal B is perpendicular to the surface exposed to air. Moreover, as a final remark, it should be pointed out that the last two spectra were observed in parallel polarization from the same micro-crystal after a crystal rotation of about 45 degrees around the Z-axis perpendicular to the crystal surface exposed to the laser beam and that the observed spectra appear to be in agreement with the group theory previsions.

The most interesting result of our experimental investigations was obtained from some unoriented rutile-type GeO_2 crystals and consisted of the observation in crossed polarization of the weak mode peaked at about 525 cm^{-1}

Table 3: Experimental and calculated Raman frequencies of rutile-type GeO_2 (in cm^{-1}). Columns (a) refer to the present work, column (b) to ref. [18], column (c) to ref. [20], column (d) to ref. [21], column (e) to ref. [23], columns (f) to ref. [24], column (g) to ref. [15]. The calculated Raman intensity (in % of the strongest mode) is reported in the square brackets and it was computed for the excitation wavelength of 647.1 nm and for rutile-type GeO_2 in polycrystalline form.

Raman modes	Exp. (a)	Exp. (b)	Exp. (c)	Exp. (d)	Exp. (e)	Exp. (f)	Th. (a)	Th. (f)	Th. (g)
B_{1g}	171	170	170	170	171	170	179 [3.0]	182	170
E_g	525	680*	–*	465*	684*	–*	529 [1.7]	546	533
A_{1g}	700	702	700	700	700	700	721 [100]	711	705
B_{2g}	873	870	873	873	873	874	870 [16.0]	869	871

*In refs. [20,24] the E_g mode was not detected, in refs. [18,23] and [21] it was tentatively (and incorrectly) guessed at about 680 and 465 cm^{-1}, respectively.

which is definitively attributed to the missing E_g mode of rutile-type GeO_2, based on the first-principles modelling discussed below. Despite its very weak relative intensity, this mode occurs as a well-shaped feature clearly separated from the A_{1g} mode peaked at 700 cm^{-1}, whose tail on the low–wave-number side has comparable intensity. Its occurrence was probed by different excitation wavelengths, *i.e.* by 454.5 nm, 488.0 nm, 514.5 nm, 568.2 nm, beside the 647.1 nm, and the related experimental spectra are reported in fig. 2, wherein each spectrum was preliminarily normalized to its full spectral intensity measured between 150 and 950 cm^{-1}.

This figure clearly shows an unusual resonant behaviour of the E_g mode *vs.* the excitation energy, so that it does not turn out observable under excitation of the blue-green laser lines. This is maybe the reason why it was never detected before, since all the reported experimental Raman studies on rutile-type GeO_2 [18–24] were carried out by means of an Ar ion laser, whose emission lines just occurs in the blue-green region of the electro-magnetic spectrum. However, the spectral evolution of the E_g mode is shared by that of the B_{1g} mode peaked at about 171 cm^{-1}, which also displays a similar, although more spectacular, intensity increase *vs.* the increase of the excitation wavelength. The occurrence of such an anomalous behaviour of both B_{1g} and E_g Raman modes of rutile-type GeO_2 *vs.* the excitation energy, far from being clarified at the state of the art, should be worth a specific dedicated study aimed at clarifying its origin.

Theoretical calculations provide further insight into the nature of Raman modes of rutile-type GeO_2, and, even more in general, of its vibrational properties. As a first step, geometry optimizations were carried out and yielded the cell parameters $a = b = 4.3445$ Å, $c = 2.8986$ Å and the ratio $a/c = 0.6672$, with oxygen cell position $x = 0.3044$. They differ from the experimental values [40] by 1.2%, 1.3%, 2.5% and 0.5%, respectively. These structural parameters have been used in the subsequent calculations reported below.

Table 1 shows the independent components of the calculated Born effective charge tensors. Both Ge and O atoms display an effective charge which is very close to their nominal ionic charges, *i.e.*, +4 for germanium and −2 for oxygen. Moreover, no large anisotropy of the Born effective charge is revealed, although there is some degree of anisotropy due to the non-zero values obtained for the non-diagonal terms of the tensors. Similar results were obtained in other rutile-type crystals, like SiO_2 and SnO_2 [41,42].

The calculated high-frequency and static dielectric tensors are displayed in table 2. To the best of our knowledge, no experimental date are available to compare with the predicted values. Anyway, our results are in good agreement with those calculated by Sevik and Bulutay [43], at least for what concerns the high-frequency dielectric tensor, and indicate a birefringence for rutile-type GeO_2 of about 0.11.

The most important computational results of the present study are the calculated frequencies and intensities of the Raman active modes listed in table 3. Our experimental detection of the E_g Raman mode at 525 cm^{-1} is corroborated both by previous theoretical calculations [15,24] and, definitely, by the present modeling, which predicts the vibrational frequency of the E_g mode at about 529 cm^{-1}. Moreover, the added value of our computational study is in the calculated relative Raman intensities (square brackets in table 3), which confirm the weak intensity of the E_g Raman mode observed in the present experiments.

Conclusions. – In this work, the vibrational dynamics of rutile-type GeO_2 (argutite) has been investigated by using micro-Raman scattering spectroscopy coupled with first-principles calculations. Polarized Raman spectra were carried out in backscattering geometry at room temperature from micro-crystalline samples either unoriented or oriented by means of a micromanipulator, which allowed to successfully detect and identify all the Raman active modes expected on the basis of the group theory. In particular, the E_g mode, incorrectly assigned or not detected in the literature, has been definitively identified by us having been unambiguously observed at 525 cm^{-1} under excitation by proper wavelengths. Moreover, it

was found that both the B_{1g} and E_g modes revealed a common, unusual resonance phenomenon *vs.* the excitation energy, which should be more deeply investigated in a future work. Finally, first-principles calculations based on the density functional theory allowed quantifying both wave number and intensity of the Raman vibrational modes, as well as other optical properties of rutile-type GeO_2. The computational results are in excellent agreement with the experimental data, corroborating the reliability of our experimental findings.

* * *

One of the authors (MG) acknowledges the financial support of the Ministero dell'Istruzione, dell'Università e della Ricerca (MIUR) within the PRIN 2010-2011 project entitled "Membrane nanocomposite avanzate ed elettrocatalizzatori innovativi per celle a combustibile ad elettrolita polimerico a lunga durata, NAMED PEM".

REFERENCES

[1] Ravindra M., Weeks R. A. and Kinser D. L., *Phys. Rev. B*, **36** (1987) 6132.
[2] Sahnoun M., Daul C., Khenata R. and Baltache H., *Eur. Phys. J. B*, **45** (2005) 455.
[3] Bielz T., Soisuwan S., Kaindl R., Tessadri R., Többens D. M., Klötzer B. and Penner S., *J. Phys. Chem. C*, **115** (2011) 9706.
[4] Deringer V. L., Lumeij M., Stoffel R. P. and Dronskowski R., *J. Comput. Chem.*, **34** (2013) 2320.
[5] Rao K. V. K., Naidu S. V. N. and Iyengar L., *J. Am. Ceram. Soc.*, **51** (1968) 467.
[6] Hazen R. and Finger L. M., *J. Phys. Chem. Solids*, **42** (1981) 143.
[7] Yamanaka T., Kurashima R. and Mimaki J., *Z. Kristallogr.*, **215** (2000) 424.
[8] Ono S., Hirose K., Nishiyama N. and Isshiki M., *Am. Mineral.*, **87** (2002) 99.
[9] Yashiro Y., Yoshiasa A., Kamishima O., Tsuchiya T., Yamanaka T., Ishii T. and Maeda H., *J. Phys. IV*, **7** (1997) 1175.
[10] Christie D. M. and Chelikowsky J. R., *Phys. Rev. B*, **62** (2000) 14703.
[11] Bertini L., Ghigna P., Scavini M. and Cargnoni F., *Phys. Chem. Chem. Phys.*, **5** (2003) 1451.
[12] Lodziana Z., Parlinski K. and Hafner J., *Phys. Rev. B*, **63** (2001) 134106.
[13] Bolzan A. A., Fong C., Kennedy B. J. and Howard C., *Acta Crystallogr. B*, **53** (1997) 373.
[14] Haines J., Léger J. M., Chateau C., Bini R. and Ulivi L., *Phys. Rev. B*, **58** (1998) R2909(R).
[15] Hermet P., Lignie A., Fraysse G., Armand P. and Papet Ph., *Phys. Chem. Chem. Phys.*, **15** (2013) 15943.
[16] Pokrovski G. S. and Schott J., *Geochim. Cosmochim. Acta*, **62** (1998) 1631.
[17] Pokrovski G. S., Roux J., Hazemann J.-L. and Testemale D., *Chem. Geol.*, **217** (2005) 127.
[18] Scott J. F., *Phys. Rev. B*, **1** (1970) 3488. See also the note added therein where a private communication from S. M. Shapiro indicates that the B_{1g} mode is at $170\,cm^{-1}$ and not at $97\,cm^{-1}$ as reported by Scott.
[19] Sharma S. K., Virgo D. and Kushiro I., *J. Non-Cryst. Solids*, **33** (1979) 235.
[20] Mammone J. F., Nicol M. and Sharma S. K., *J. Phys. Chem. Solids*, **42** (1981) 379.
[21] Gillet P., Le Cléac'h A. and Madon M., *J. Geophys. Res.*, **95** (1990) 21635.
[22] Sato T., *Pramana - J. Phys.*, **38** (1992) 355.
[23] Mernagh T. P. and Liu L.-g., *Phys. Chem. Miner.*, **24** (1997) 7.
[24] Kaindl R., Többens D. M., Penner S., Bielz T., Soisuwan S. and Klötzer B., *Phys. Chem. Miner.*, **39** (2012) 47.
[25] Damen T. C., Porto S. S. P. and Tell B., *Phys. Rev.*, **142** (1966) 570.
[26] Giarola M., Sanson A., Monti F., Mariotto G., Bettinelli M., Speghini A. and Salviulo G., *Phys. Rev. B*, **81** (2010) 174305.
[27] Giarola M., Sanson A., Rahman A., Mariotto G., Bettinelli M., Speghini A. and Cazzanelli E., *Phys. Rev. B*, **83** (2011) 224302.
[28] Sanson A., Giarola M., Bettinelli M., Speghini A. and Mariotto G., *J. Raman Spectrosc.*, **44** (2013) 1411.
[29] Dovesi R., Orlando R., Erba A., Zicovich-Wilson C. M., Civalleri B., Casassa S., Maschio L., Ferrabone M., De La Pierre M., D'Arco P., Noel Y., Causa M., Rerat M. and Kirtman B., *Int. J. Quantum Chem.*, **114** (2014) 1287.
[30] Ruiz E., Llunell M. and Alemany P., *J. Solid State Chem.*, **176** (2003) 400.
[31] Muscat J., Harrison N. M. and Thornton G., *Phys. Rev. B*, **59** (1999) 2320.
[32] Scaranto J. and Giorgianni S., *J. Mol. Struct.: THEOCHEM*, **858** (2008) 72.
[33] Dirac P. A. M., *Proc. Cambridge Philos. Soc.*, **26** (1930) 376.
[34] Vosko S. H., Wilk L. and Nusair M., *Can. J. Phys.*, **58** (1980) 1200.
[35] Maschio L., Kirtman B., Rérat M., Orlando R. and Dovesi R., *J. Chem. Phys.*, **139** (2013) 164101.
[36] Monkhorst H. and Pack J., *Phys. Rev. B*, **13** (1976) 5188.
[37] Zicovich-Wilson C. M., Pascale F., Roetti C., Saunders V. R., Orlando R. and Dovesi R., *J. Comput. Chem.*, **25** (2004) 1873.
[38] Pascale F., Zicovich-Wilson C. M., Gejo F. L., Civalleri B., Orlando R. and Dovesi R., *J. Comput. Chem.*, **25** (2004) 888.
[39] Loudon R., *Adv. Phys.*, **13** (1964) 423.
[40] Baur W. H. and Khan A. A., *Acta Crystallogr. B*, **27** (1971) 2133.
[41] Lee C. and Gonzie X., *Phys. Rev. Lett.*, **72** (1994) 1686.
[42] Borges P. D., Scolfaro L. M. R., Leite Alves H. W. and da Silva E. F. jr., *Theor. Chem. Acc.*, **126** (2010) 39.
[43] Sevik C. and Bulutay C., *J. Mater. Sci.*, **42** (2007) 6555.